ANL/NT/CP-98162-A

MICROSTRUCTURAL DEVELOPMENT IN WASTE FORM ALLOYS CAST FROM IRRADIATED CLADDING RESIDUAL FROM THE ELECTROMETALLURGICAL TREATMENT OF EBR-II SPENT FUEL[1]

by

Dennis D. Keiser, Jr.

Argonne National Laboratory-West
P. O. Box 2528
Idaho Falls, ID 83403-2528

Paper to be Published in the Proceedings of the GLOBAL '99 International Conference on

Future Nuclear Systems

Jackson Hole, Wyoming

August 30-September 2, 1999

---

[1] Work supported by the U.S. Department of Energy, Reactor Systems, Development Technology, under Contract W-31-109-ENG-38.

DISCLAIMER

Portions of this document may be illegible in electronic image products. Images are produced from the best available original document.

DISCLAIMER

MICROSTRUCTURAL DEVELOPMENT IN WASTE FORM ALLOYS CAST FROM IRRADIATED CLADDING RESIDUAL FROM THE ELECTROMETALLURGICAL TREATMENT OF EBR-II SPENT FUEL

Dennis D. Keiser, Jr.
Argonne National Laboratory-West
P. O. Box 2528
Idaho Falls, Idaho 83403
(208) 533-7298

ABSTRACT

A metallic waste form alloy that consists primarily of stainless steel and zirconium is being developed by Argonne National Laboratory to contain metallic waste constituents that are residual from an electrometallurgical treatment process for spent nuclear fuel. Ingots have been cast in an induction furnace in a hot cell using actual, leftover, irradiated, EBR-II cladding hulls treated in an electrorefiner. The as-cast ingots have been sampled using a core-drilling and an injection-casting technique. In turn, generated samples have been characterized using chemical analysis techniques and a scanning electron micrroscope equipped with energy-dispersive and wavelength-dispersive spectrometers. As-cast ingots contain the predicted concentration levels of the various constituents, and most of the phases that develop are analogous to those for alloys generated using non-radioactive surrogates for the various fission products.

I. INTRODUCTION

Argonne National Laboratory is developing an electrometallurgical treatment for spent nuclear fuel [1], and the initial demonstration of this technology is being conducted in the Fuel Conditioning Facility (FCF) using fuel from the EBR-II reactor, located in Idaho Falls, ID. Most of the fuel being treated is made up of driver fuel elements. These elements consist of U-10Zr[1] fuel and either Type 316[2] or D9[3] stainless steel cladding. Some blanket fuel elements are being treated that consist of U metal and Type 304[4] stainless steel. Most of the driver fuel has been irradiated to around 8.0 at.% burnup[5]. The blanket fuel has seen much lower burnup.

In the electrometallurgical treatment process, fuel elements are chopped into ~0.64 cm segments and placed into stainless steel baskets, which in turn are placed into an electrorefiner (at the anode position). In the electrorefiner, the anode baskets sit in eutectic LiCl-KCl eutectic salt heated to ~500°C. The uranium is electrolytically dissolved from the stainless steel (SS) cladding segments and is deposited onto a stainless steel mandrel (the cathode). The active fission products (e.g., Ba, Na, Cs, etc.) are dissolved into the salt, and later extracted and placed into a ceramic waste form [2]. The material remaining in the anode baskets, including cladding segments (hulls), zirconium from the original U-10Zr alloy fuel, noble metal fission products[6] (NMFP), and some residual uranium, is subsequently cast to form an ingot. The ingot is called the metal waste form (MWF) and is to be disposed of in a geologic repository [3]. The nominal composition of the alloy is SS-15Zr[7].

Ingots have been cast in an induction furnace located in a hot cell using actual irradiated materials from the electrorefiner [4]. These ingots have been sampled using a core-drilling (CD) and injection-casting (IC) technique. In turn, the generated samples have been characterized using chemical analyses and a scanning electron microscope (SEM) equipped with energy-dispersive and wavelength-dispersive spectrometers (EDS/WDS).

This paper describes the composition of and microstructural development in recent as-cast ingots. The microstructures that develop are, in turn, compared to those observed for MWF ingots generated using surrogates, for the various fission products, and depleted uranium. It is these spiked ingots that are receiving the bulk of the property testing to show how a MWF would perform in a geologic repository. It is important to assure

---

[1] All compositions are listed in wt.%, unless otherwise stated.

[2] Type 316SS has a nominal composition, in wt.%, of 16.3Cr-10.5Ni-2.1Mo-1.5Mn-0.7Si-0.05C-0.06N-0.008O-bal Fe.

[3] Type D9SS has a nominal composition, in wt.%, of 13.5Cr-15.5Ni-2.0Mo-2.0Mn-0.75Si-0.25Ti-0.04C-bal Fe.

[4] Type 304SS has a nominal composition, in wt.%, of 18.3Cr-8.2Ni-1.5Mn-0.4Si-0.3Mo-0.3Cu-0.2Co-0.3P-0.02S-0.08N-0.08C-bal Fe.

[5] This term describes the amount of heavy atoms fissioned.

[6] These elements are so named since they are noble to the electrorefining process, and they include elements like Ru Tc, Te, Rh, Rb, Pd, Ti, Se, Sn, Ag, Sb, V, Cu, Nb, etc.

[7] SS is used to account for the components found in stainless steels.

that the microstructures of the tested spiked alloys and those of the "actual" alloys are analogous. This will add credibility to the performance data derived from the doped MWF alloys.

II. EXPERIMENTAL

After electrorefining, the anode baskets are removed from the electrorefiner, and there is LiCl-KCl eutectic salt left adhering to the anode baskets and the material in the anode baskets. This salt must be removed before the metallic waste can be cast into an MWF ingot because the salt reacts with the yttria crucibles that are used for casting. Salt removal is accomplished in a distillation furnace, under vacuum, at a temperature of ~1100°C. Once the salt is removed, the metallic charge is loaded into an yttria crucible and cast into an ingot using an induction furnace, a casting temperature of 1600°C, and a hold time of around 2 hours. The alloy is slow-cooled, and the solidified, disk-shaped ingot (~2.5 cm thick x ~21.6 cm diameter) is removed from the crucible.

Samples are produced from MWF ingots in one of two ways. Either an IC technique is used to sample the alloy when it is molten, or a CD technique is used to generate samples from the solidified, as-cast ingot. The IC technique consists of vacuum-injecting molten alloy into quartz molds to produce pins ~0.43 cm diameter that can be subsequently sliced into small sections that can be used for chemical or microstructural analyses. CD consists of generating 0.33 cm or 1.3 cm diameter cores from the as-cast ingots, using a drill-press and either tool steel or diamond-layered tool steel drill bits under flowing water or in dry conditions.

Both transverse and longitudinal slices of the core-drilled and injection-cast samples are analyzed using an SEM. Initially, the samples are mounted in an acrylic mount and ground and polished through 1-μm. Secondary electron and backscattered electron micrographs are taken of the microstructures using either an AMRAY SEM or a Zeiss DSM960A SEM, operated at 20 or 30 kV accelerating voltages. Energy-dispersive spectroscopy and wavelength-dispersive spectroscopy analyses are performed using ISIS Link software.

Chemical analyses of the monolithic samples cut from the injection-cast and core-drilled pins from various ingots are performed by dissolving samples in acid solutions and measuring the various components in the solutions using a variety of techniques, e.g., mass spectrometry, ICP-atomic emission spectrometry, and gamma spectrometry. The components that are measured include the major stainless steel components, Zr, Y (from the casting crucible), impurities (C, O, N), some of the prevalent NMFPs (Ru, Pd, and Tc), and actinides (U, Pu, and Np).

III. RESULTS

A. Chemical Analyses of MWF Samples

Table 1 enumerates the chemical analyses results for CD samples taken from the four most recent MWF ingots cast in the FCF. They have been designated CFMW05, CFMW06, CFMW07, and CFMW08. Ingot CFMW05 contained Type 316SS cladding hulls from driver fuel elements; ingots CFMW06 and CFMW07 contained

Table 1. Chemical Analyses Results* for CD Samples From MWF Ingots CFMW05, CFMW06, CFMW07, and CFMW08.

Analyte	Units	05	06	07	08
Total U	wt.%	9.34	2.36	0.93	NA**
Zr	wt.%	14.13	10.60	16.41	13.5
Fe	wt.%	45.00	61.88	57.34	61.3
Cr	wt.%	11.57	13.72	11.61	16.1
Ni	wt.%	7.48	11.73	13.21	8.6
Mo	wt.%	1.54	2.39	2.57	0.18
Mn	wt.%	1.05	1.68	1.75	1.2
Cd	ppm	110	ND***	18	ND
Y	ppm	23	4	68	90
Pd	wt.%	0.08	0.11	0.12	NA
Tc	wt.%	0.11	0.32	0.31	ND
Ru	wt.%	0.17	0.66	0.62	ND
Mn54	ppb	228	8.2	154	NA
Co57	ppb	ND	ND	ND	NA
Co60	ppb	383	191	457	NA
Nb95	ppb	ND	ND	ND	NA
Ru106	ppb	3123	420	2999	NA
Sb125	ppb	3212	2356	5600	NA
Cs137	ppb	1425	44	ND	NA
Ce144	ppb	8.5	ND	5.2	NA
U234	% of U	0.65	0.67	0.54	NA
U235	% of U	58.02	61.01	47.61	NA
U236	% of U	2.12	2.11	1.55	NA
U238	% of U	39.22	36.21	50.30	NA
Np237	ppm	ND	9	10	11.5
Total Pu	ppm	32	7	4	NA

* Compositions are averages of multiple samples, where the agreement was good between the various samples (i.e., low standard deviations); the highest errors are associated with the Fe concentrations. **NA: Not Analyzed; *** ND: Not Detected (below detection limits); (Other elements looked for and not detected include: Li, K, Na, Nd, Ce, Zr95, Cs134, Eu154, Rh106, Eu155, and Ta182)

D9SS cladding hulls, from driver fuel elements; and ingot CFMW08 contained Type 304SS cladding hulls from blanket fuel elements. Chemical analyses results for the IC samples taken from ingots CFMW05, CFMW06, and CFMW07 are shown in Table 2.

Table 2. Chemical Analyses Results* for IC Samples From MWF Ingots CFMW05, CFMW06, and CFMW07.

Analyte	Units	05	06	07
Total U	wt.%	9.27	2.48	0.94
Zr	wt.%	12.65	8.75	14.88
O	ppm	360	248	1563
C	ppm	200	747	529
N	ppm	3	12	13
Fe	wt.%	49.03	53.20	56.58
Cr	wt.%	12.65	11.73	11.30
Ni	wt.%	8.25	10.33	12.95
Mo	wt.%	1.88	2.00	2.49
Mn	wt.%	1.26	1.53	1.69
Cd	ppm	138	177	175
Si	wt.%	0.50	0.95	1.60
Y	ppm	550	63	ND**
Pd	wt.%	0.09	0.13	0.11
Tc	wt.%	0.11	0.28	0.32
Ru	wt.%	0.17	0.62	0.59
Mn54	ppb	327	14	181
Co57	ppb	2	ND	ND
Co60	ppb	399	200	484
Nb95	ppb	0.1	ND	ND
Ru106	ppb	4130	635	3475
Sb125	ppb	3598	2891	5975
Cs137	ppb	182	ND	ND
Ce144	ppb	ND	0.2	ND
U234	% of U	0.65	0.67	0.54
U235	% of U	58.03	60.95	47.58
U236	% of U	2.12	2.11	1.55
U238	% of U	39.21	36.28	50.30
Np237	ppm	499	ND	ND
Total Pu	ppm	42	3	3

* Compositions are averages of multiple samples, where the agreement was good between the various samples (i.e., low standard deviations); Fe has the highest errors. ** ND: Not Detected (below detection limits); (Other elements looked for and not detected include: Li, K, Na, Nd, Ce, Zr95, Cs134, Eu154, Rh106, Eu155, and Ta182)

The results show that the as-cast ingots had U concentrations that varied from ~1.0 wt.% in CFMW07 to ~9.0 wt.% in CFMW05 and Zr concentrations that varied from ~9.0 to 10.0 wt.% in CFMW06 to ~15.0 wt.% in CFMW07. Of the NMFPs that were analyzed for, Ru was observed in the highest concentrations (from ~0.2 wt.% in CFMW05 to ~0.6 wt.% in CFMW06); Pd was observed to be the least prevalent (around 0.1 wt.% in all alloys).

By comparing the chemical analyses results for the MWF ingots when they were molten (Table 2) with the results for the MWF ingots after they had solidified (Table 1), it can be concluded that both sampling techniques give similar results. It should be noted that the data for the individual core-drilled samples that make-up the averages shown in Table 1 exhibited relatively good agreement. Therefore, since the CD samples were taken at different ingot locations, the ingots appear to be homogeneous.

B. Microstructural Analysis of IC Samples

A typical microstructure observed for a cross-sectioned injection-cast sample is presented in Figure 1. The major features that comprise the microstructue include: (1) a dark-contrasted Fe solid solution phase; (2) a medium-contrasted $Zr(Fe,Cr,Ni)_{2+x}$ intermetallic phase, and (3) a bright-contrasted, actinide-enriched $Zr(Fe,Cr,Ni)_{2+x}$ intermetallic phase. Due to the fine microstructure, where the various phases are around 1 μm in size, phase compositions could not be determined. SEM/EDS/WDS requires that phases are larger than 2 μm before their compositions can be definitively determined.

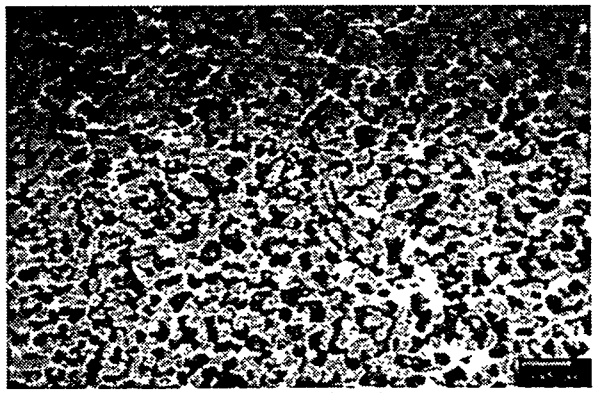

Figure 1. SEM micrograph of a CFMW05 IC sample. The darkest phase is an Fe solid solution phase; the medium-contrasted phase is $Zr(Fe,Cr,Ni)_{2+x}$, and the brightest-contrast areas are enriched in U.

C. Microstructural Analysis of CD Samples

Figure 2 shows an example of an ingot that has been core-drilled. The smaller diameter cores are employed for microstructural characterization. The microstructure of a

core-drilled sample taken from the SS-15Zr-9U alloy, CFMW05, is presented in Figure 3. It is representative of the microstructures observed for the various MWF alloys

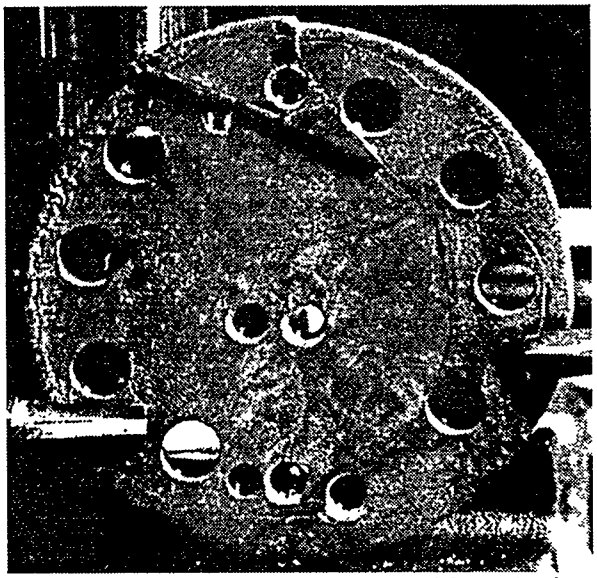

Figure 2. Picture of ingot CFMW06 (~21.6 cm diameter) after core-drilling was performed in the FCF.

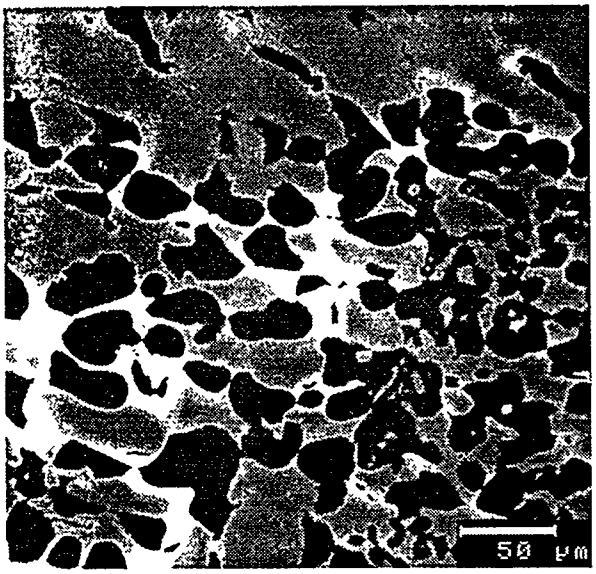

Figure 3. SEM micrograph of microstructure observed for CD sample taken from CFMW05. The darkest regions are the Fe solid solution phase; the medium-contrast phase is the $Zr(Fe,Cr,Ni)_{2+x}$, with the brightest regions in this phase being enriched in U.

cast in FCF. This eutectic alloy microstructure comprises three major phases: an Fe solid solution phase (austenite and sometime ferrite), a $Zr(Fe,Cr,Ni)_{2+x}$ phase, and a high-uranium region in the $Zr(Fe,Cr,Ni)_{2+x}$ phase that appears bright in a SEM micrograph. This microstructure is observed for all SS-(9-15)Zr-based alloys that contain actinides. Increasing the amount of uranium in the SS-15Zr alloy results in a higher volume fraction of the high-contrast, high-actinide regions in the $Zr(Fe,Cr,Ni)_{2+x}$ phase. No mass segregation of uranium into discrete phases is observed.

Some minor phases have been identified in the various as-cast MWF ingots. One of these phases is shown in Figure 4. This phase contains Te and Se combined with either U or Zr. It appears adjacent to the $Zr(Fe,Cr,Ni)_{2+x}$ phase, and in many cases a Zr-rich phase

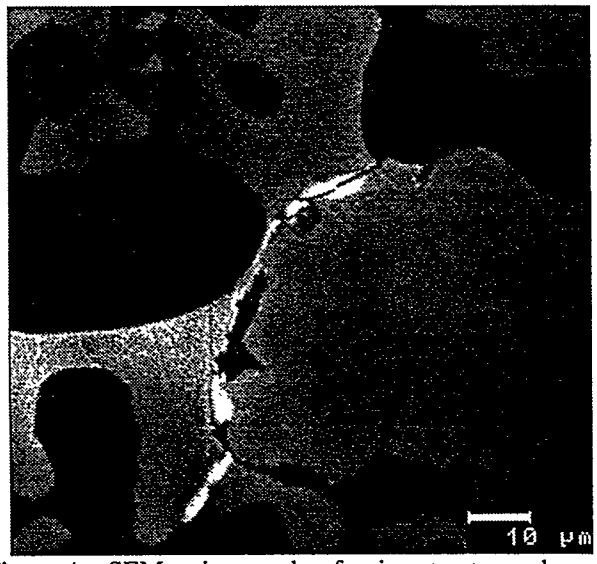

Figure 4. SEM micrograph of microstructure observed for a CD sample taken from CFMW05. Bright particles contain U and Te.

Figure 5. SEM micrograph of a CFMW06 CD sample. The darkest phase is ferrite; the medium-contrast phase is austenite; and the largest, bright-contrasted phase is

$Zr(Fe,Cr,Ni)_{2+x}$. Isolated phases are present on the ferrite/austenite boundaries (arrows).
is in close proximity. Other minor phases appear on ferrite/austenite boundaries (see Figure 5), while a final minor phase forms as micron- sized U(Mo,Ru) particles. Not all of these phases have been observed in every alloy.

Some typical compositions of the phases observed in the various ingots are enumerated in Table 3. Though not listed in Table 3, phases on ferrite/austenite boundaries and U-Te particles were observed in the microstructure of CFMW06, but reliable compositions could not be determined due to the small size of the phases. For CFMW08, Te or Se-containing phases were not observed, but instead, micron-sized U particles that contained Mo and Ru were detected. Due to the low concentration levels for elements like Ru, Pd, and Tc in the MWF ingots (see Table 1), not all alloy constituents could be quantified using SEM/EDS/WDS. The presence of these elements in certain phases could be confirmed though, using SEM/WDS to resolve X-ray peaks for the various constituents.

In most cases, the various MWF alloy constituents favor specific alloy phases. Of the NMFPs, Ru is found to favor the $Zr(Fe,Cr,Ni)_{2+x}$ phase, while Tc favors the Fe solid solution phases, i.e. ferrite and austenite. The phases preferred by other measurable alloy constituents are depicted in Table 4.

Table 3. Typical Phase Compositions for MWF Ingots.

		Phase Composition (at.%)*								
Ingot	Phase	Fe	Cr	Ni	Zr	Mn	Mo	Si	U	Other
CFMW05	Ferrite	66.1	27.9	2.9	neg.**	2.0	1.1	neg.	neg.	
	U-rich $Zr(Fe,Cr,Ni)_{2+x}$	44.9	2.8	24.7	3.2	1.7	neg.	neg.	22.6	
	U-Te phase	5.9	4.2	neg.	neg.	neg.	neg.	neg.	37.9	52.0Te
	Zr-rich	7.0	1.7	1.2	89.4	neg.	neg.	neg.	1.3	
	Zr_6Fe_{23}	58.1	10.2	12.0	16.8	1.3	0.3	neg.	1.4	
CFMW06	Ferrite	66.6	25.1	3.9	neg.	1.5	2.1	0.9	neg.	
	Austenite	70.7	17.3	8.3	neg.	1.9	1.1	0.7	neg.	
	$Zr(Fe,Cr,Ni)_{2+x}$	45.4	5.4	20.7	22.2	1.8	0.7	2.7	1.2	
CFMW07	Ferrite	66.6	25.0	3.8	neg.	1.7	2.5	0.7	neg.	
	Austenite	69.5	16.6	8.7	neg.	2.8	1.3	1.0	neg.	
	$Zr(Fe,Cr,Ni)_{2+x}$	45.8	5.8	20.1	21.7	1.9	0.3	3.2	1.1	
	FAI*** phase 1	62.3	27.0	3.1	neg.	2.0	3.9	1.5	neg.	
	FAI phase 2	65.4	16.1	10.4	3.5	1.8	0.9	1.7	neg.	
	U-Te phase	4.6	neg.	neg.	neg.	neg.	neg.	neg.	39.1	56.3Te
	Zr-Te phase (Se-rich)	neg.	neg.	neg.	66.1	neg.	neg.	neg.	1.0	14.0Te 19.8Se
	Zr-Te phase (Te-rich)	neg.	neg.	neg.	65.2	neg.	neg.	neg.	neg.	22.5Te 12.3Se
CFMW08	Ferrite	70.2	22.8	4.4	neg.	2.1	0.3	neg.	neg.	
	$Zr(Fe,Cr,Ni)_{2+x}$	49.0	4.5	20.7	23.1	1.9	neg.	neg.	1.8	
	U-rich $Zr(Fe,Cr,Ni)_{2+x}$	42.7	2.2	25.7	8.8	1.7	neg.	neg.	18.4	
	Zr_6Fe_{23}	56.5	7.6	14.7	18.2	0.9	neg.	1.0	1.6	
	Zr-S	6.5	1.0	2.4	73.7	0.4	neg.	neg.	neg.	16.0S
	Zr-rich	neg.	neg.	neg.	99.9	neg.	neg.	neg.	neg.	

* Error is ±3%; ** neg.- negligible; *** Ferrite Austenite Interface

Table 4. Partitioning Behavior of MWF Alloy Constituents Between Alloy Phases.

Alloy Component	Favored Phase
Fe	Fe solid solution
Ni	$Zr(Fe,Cr,Ni)_{2+x}$
Cr	Fe solid solution
Mo	Both phases equally
Mn	Both phases equally
Si	$Zr(Fe,Cr,Ni)_{2+x}$
S	Minor phase
Zr	$Zr(Fe,Cr,Ni)_{2+x}$
U	$Zr(Fe,Cr,Ni)_{2+x}$
Se	Minor phase
Te	Minor phase
Ru	$Zr(Fe,Cr,Ni)_{2+x}$
Tc	Fe solid solution

IV. DISCUSSION

A. Ingot Compositions

How the electrorefiner is operated determines how much U and Zr will be left behind in the anode baskets [5], which will affect the composition of the MWF. Typically, the electrorefiner is run to try and remove as much U from the cladding hulls as possible (to be deposited on the cathode), while leaving most, if not all, of the Zr behind with the cladding hulls (to be incorporated into the MWF). The Zr is usually left behind as layers on the cladding hulls [4]. These cladding hulls are then cast into MWF ingots that are being qualified to accommodate a range of Zr concentrations. The allowable range is 5 to 20 wt.% Zr for the alloy. Typically MWF ingots are cast with a composition around 15 wt.% Zr, thereby allowing for local variations in concentrations that will stay within the overall 5 to 20 wt.% range.

In order to maximize the Zr left with the cladding hulls, it is necessary to also leave some small amount of U. As shown in Tables 1 and 2, up to 9.0 wt.% U has been left with the cladding hulls. By comparing the microstructure of the MWF ingot that contains 9.0 wt.% U (CFMW05) with the one containing negligible U (CFMW07), it has been concluded that there is no major change in the nominal microstructure of the MWF when increasing amounts of U are added, just an increase in the amount of U-rich regions in the $Zr(Fe,Cr,Ni)_{2+x}$ phase.

For the NMFPs, most of those contained in the original fuel are expected to remain with the cladding hulls, since the NMFPs are noble to the process. However, some NMFPs could possibly escape the mesh-screened baskets. The NMFPs are observed as isolated particles in the original as-irradiated fuel [6], and as the fuel is dissolved, some particles could possibly escape the mesh-screened baskets, float in the eutectic salt, and eventually deposit somewhere in the electrorefiner. This does not seem to have happened to a large extent. Calculations have been performed whereby the amount of NMFPs in a representative EBR-II fuel assembly after ~8.0 at.% burnup has been calculated using techniques described in [7]. The Ru, Pd, and Tc concentrations in a fuel assembly were calculated to equal 0.32, 0.007, and 0.14 wt.%, respectively. These concentration levels agree with the Ru, Pd, and Tc concentrations measured for the MWF ingots cast from the residual metallic waste (see Tables 1 and 2).

Te and Se are noble to the electrorefining process. Yet, they should not be present in the MWF. In the original fuel, at ~8.0 at.% burnup, Te and Se are present in concentrations of approximately 0.009 and 0.002 wt.%, respectively. However, during the casting process they should volatize away. The boiling points for Te and Se are 988°C and 685°C, respectively [8], and the cladding hulls are exposed to temperatures of 1100°C and 1600°C in the distillation furnace and casting furnace, respectively. Yet, based on the microstructures for the MWF ingots described above, Te and Se form intermetallic phases with U and Zr. These phases do not melt until they are exposed to high temperatures, based on available phase diagrams [9] (e.g., the binary U-Te phase melts at 1740°C). Due to the large amount of intermetallics that want to form between Te and Se with U and Zr (e.g., nine for U and Te), it appears that there is a large driving force for these phases to form in the MWF. Once they do, they do not volatize away during high temperature processing, leaving Te and Se behind in the ingots.

Looking at the measured amounts of impurities (see Tables 1 and 2), the C, O, N concentration levels in the MWF ingots are reasonably low. This suggests that the amount of slag that develops on MWF ingots should be small. The completed microstructural analyses of longitudinally-cut, CD samples taken from the ingots confirm this. Little evidence of any developed slag/oxide layers was observed in the regions of the CD samples that corresponded to the top of the as-cast MWF ingots.

B. Microstructural Development

As reported in the literature, the microstructure that develops in SS-15Zr alloys follows what would be expected based on the Fe-Zr phase diagram [9]. Two major phases develop: the $Zr(Fe,Cr,Ni)_{2+x}$ phase and the Fe solid solution phase. Close to 50 volume percent of

each phase comprise the microstructure of the SS-15Zr alloy. The amount of ferrite relative to austenite depends on the Ni content in the starting stainless steel and the Zr content of the SS-Zr alloy [3]. Austenite is observed to contain more Ni and less Cr than does ferrite. The $Zr(Fe,Cr,Ni)_{2+x}$ phase is enriched in Ni, which can reduce the amount of austenite that will form, since Ni stabilizes austenite. So, the more $Zr(Fe,Cr,Ni)_{2+x}$ that forms (when more Zr is added) the less austenite that will form. As a result, below 15 wt.% Zr the Fe solid solution phase is a mixture of ferrite and austenite, while at higher Zr concentrations, ~15 wt.% Zr, the Fe solid solution phase is primarily ferrite.

Another Zr-Fe phase that develops in SS-Zr alloys is the $Zr_6(Fe,Cr,Ni)_{23}$ phase. This phase is kinetically slow to develop in MWF alloys [10], and typically between 1 and 5% of this phase is found in SS-15Zr. Such amounts of this phase are observed in the alloys described in this paper.

The other minor phases that have been observed in the MWF ingots discussed in this paper, including the Zr-S phase, the Zr-rich phase, ferrite/austenite boundary phases, and micron-sized U(Mo,Ru) phases, do not contain appreciable actinides and/or NMFPs, and are present in very small amounts. Zr-S probably forms due to the S present in cladding materials, like Type 304SS and 316SS. The Zr-rich phase forms in areas whether other phases (e.g., $Zr_6(Fe,Cr,Ni)_{23}$, Zr-S, U-Te) have formed. The U(Mo,Ru) particles that appear in ingot CFMW08 seem to replace the Te and Se phases that were observed in the other ingots. These phases are very small in size (<1 μm) and amount, because the Mo and Ru concentration levels in CFMW08 are very low. CFMW08 was cast out of cladding hulls from blanket fuel elements, instead of the driver fuel element cladding that the other ingots were generated from. So, instead of the original 8.0 at.% burnup, U-10Zr alloy fuel that contained small amounts of Te and Se, the starting fuel in the anode baskets of the electrorefiner was very low burnup U with negligible fission products. Therefore, when the residual material from the anode baskets was cast into MWF ingots, small U(Mo,Ru) particles apparently formed instead of Te or Se-containing phases.

C. Partitioning of Alloy Constituents

Of primary interest for this study, in terms of how alloy constituents partition between alloy phases, is how the actinides (primarily U) and Tc behave in the MWF alloys. Since the primary goal when developing a waste form is to contain the waste constituents for geologic timeframes, it is preferable that these components not segregate into waste constituent-enriched phases. In some cases, these types of phases may be locally attacked if the alloy is exposed to an aqueous environment. Instead, the waste constituents should be homogeneously distributed throughout the waste form.

In the case of the MWF, Tc-enriched phases are not observed. Tc is a NMFP with a half-life of 2.15×10^5 years, and it is found to be mobile in water, as the pertechnetate ion [11]. Reportedly, when Tc is contained as an oxide in a simulated glass waste form, it leaches out into aqueous solutions at a relatively fast rate [12]. Whereas, Tc is in the metallic state in the MWF, and it is homogeneously distributed throughout the alloy and is found in all alloy phases, with a slight preference for the Fe solid solution phases. The Tc leaching rates in the MWF alloys, with such an even distribution of Tc, prove to be low when samples are tested in aqueous environments [13]. In addition, the other NMFPs display low leach rates from doped MWF alloys exposed to aqueous solutions [14].

With regards to the actinides (primarily U), the $Zr(Fe,Cr,Ni)_{2+x}$ phase is observed to heterogeneously accommodate U in the MWF. Up to 22.0 at.% U has been observed in local areas of this phase, while other areas contain as little as 2.0 at.% U. The $Zr(Fe,Cr)_{2+x}$ phase consists of different polytypes (C14, C15, and C36), with different crystal strucutres [14]. It is suspected that the U is favoring one of the polytypes of the $Zr(Fe,Cr)_{2+x}$ phase that have been observed in MWF alloys. MWF ingots doped with actinides have been heat-treated at high temperatures to determine if the observed alloy microstructures were stable. It was concluded that these alloys, which had microstructures like the ones described for the MWF alloys discussed in this paper, were relatively stable. In actual leaching tests, where U-containing MWF alloys were exposed to aqueous environments, the rate at which U leached from MWF samples was observed to be low [13].

D. Comparisons to Surrogate Alloys

Results from investigations of microstructural development in MWF alloys doped with NMFP surrogates and actual actinides have been reported [15]. The structures that develop in these alloys are analogous to those structures reported for the SS-Zr alloys discussed in this paper. Only the Te-containing, Se-containing, and U(Mo,Ru) phases found in the present study have not been observed in doped MWF alloys (none of the doped MWF alloys contained Te or Se). As a result, MWF ingots generated from actual process waste are expected to behave quite similarly to doped MWF ingots in performance tests (i.e., leaching tests, corrosion tests, etc.), since they have almost identical microstructures.

V. CONCLUSIONS

Based on the results of a microstructural investigation of MWF alloy ingots that were cast in an induction

furnace in the FCF at ANL-West, the following conclusions can be drawn:

1. Homogeneous waste form ingots can be generated from metallic waste residual from the electrometallurgical treatment of EBR-II spent fuel using an induction furnace located in a hot cell.

2. Injection-casting and core-drilling techniques can be employed to produce samples for composition and microstructural development determination.

3. Injection-cast samples exhibit relatively fine microstructures compared to those observed for core-drilled samples.

4. The major phases that develop in as-cast MWF ingots include the $Zr(Fe,Cr,Ni)_{2+x}$ phase and the Fe solid solution phase. Minor phases include: the $Zr_6(Fe,Cr,Ni)_{23}$, Zr-S, Zr-rich, U(Te,Se), Zr(Te,Se), and U(Mo,Ru) phases.

5. Microstructural development in MWF ingots cast in the FCF is analogous to what is observed for MWF ingots doped with NMFPs and actinides. As a result, the behavior of FCF MWF ingots in various performance tests is expected to be analogous to what has been observed for MWF ingots doped with NMFPs and actinides.

ACKNOWLEDGMENTS

This work was supported by the U. S. Department of Energy, Office of Nuclear Energy, Science, and Technology, under contract W-31-109-Eng-38. ANL-West Analytical Laboratory personnel are acknowledged for their chemical analyses of MWF samples. Acknowledgment is given to B. R. Westphal, S. G. Johnson, T. P. O'Holleran, and R. N. Elliott for their assistance in sampling MWF ingots and in conducting SEM analysis.

REFERENCES

1. J.E. Battles, J.J. Laidler, C.C. McPheeters, and W.E. Miller, "Pyrometallurgical Process for Recovery of Actinide Elements," *Actinide Processing: Methods and Materials*, ed. B. Mishra and W.A. Averill, p. 135-151, The Minerals, Metals, & Materials Society, Warrendale, PA, (1994).

2. J. P. Ackerman, T. R. Johnson, L. S. H. Chow, E. L. Carls, W. H. Hannum, J. J. Laidler, "Treatment of Wastes in the IFR Fuel Cycle," *Prog. Nucl. Energy*, **31**, 141 (1997).

3. S. M. McDeavitt, D. P. Abraham, and D. D. Keiser, Jr., "SS-Zr Waste Forms from the Treatment of Spent Nuclear Fuel," *JOM*, **49(7)**, 29-32 (1997).

4. D. D. Keiser, Jr. and B. R. Westphal, "Consolidation of Cladding Hulls From the Electrometallurgical Treatment of Spent Fuel," in: *Proceedings of the Third Topical Meeting on DOE Spent Nuclear Fuel and Fissile Materials Management*, Charleston, SC, September 8-11, 1998, p. 668, ANS, La Grange Park, IL (1998).

5. T. C. Totemeier and R. D. Mariani, "Morphologies of Uranium and Uranium-Zirconium Electrodeposits," *J. Nucl. Mater.*, **250**, 131 (1997).

6. G. L. Hofman, "Metallic Fast Reactor Fuels," in: R. W. Cahn, P. Haasen, E. J. Kramer (Eds.), Materials Science and Technology: A Comprehensive Treatment, vol. 10, VCH Publishers, New York, p. 1 (1994).

7. R. D. McKnight, J. A. Stillman, B. J. Toppel, and H. S. Khali, "Validation and Application of a Physics Database for Fast Reactor Fuel Cycle Analysis," *Proc. Topical Meeting on Advances in Reactor Physics*, Vol. 1, Knoxville, TN, April 11-15, 1994, p. 150, ANS, La Grange Park, IL, (1994).

8. C. J. Smithells, *Metals Reference Book*, p. 188, Butterworth and Co., Boston, Mass. (1978).

9. T. B. Massalski, Ed., *Binary Alloy Phase Diagrams*, Vol. II, ASM International, Materials Park, OH (1990).

10. D. P. Abraham, J. W. Richardson, Jr., and S. M. McDeavitt, "Formation of the $Fe_{23}Zr_6$ Phase in an Fe-Zr Alloy," *Scripta Mater.*, **37(2)**, 239 (1997).

11. M. Kumata and T. T. Vandergraaf, "Technetium Behaviour Under Deep Geological Conditions," *Radioactive Waste Management and the Nuclear Fuel Cycle*, **17(2)**, 107 (1993).

12. D. J. Bradley, C. O. Harvey, R. P. Turcotte, "Leaching of Actinides and Technetium from Simulated High-Level Waste Glass," *PNL-3152* (1979).

13. S. G. Johnson, D. D. Keiser, M. Noy, T. O'Holleran, and S. M. Frank, "Microstructure and Leaching Characteristics of a Technetium Containing Metal Waste Form," *Mat. Res. Soc. Symp. Proc.* (1998) accepted for publication.

14. S. M. McDeavitt, D. P. Abraham, and J. Y. Park, "Evaluation of SS-Zr Alloys as High-Level Nuclear Waste Forms," *J. Nucl. Mater.*, **257**, 21 (1998)

15. D. D. Keiser, Jr. and S. M. McDeavitt, "Actinide-Containing Metal Disposition Alloys," in: *Proc. Third Topical Meeting on DOE Spent Nuclear Fuel and Fissile Materials Management*, Reno, NV, June 16-20, 1996, p. 178, ANS, La Grange Park, IL (1996).